Separation Science and Technology
Publication details, including instructions for authors and subscription information:
http://www.informaworld.com/smpp/title~content=t713708471

Studies on Palladium Membrane Reactor for Dehydrogenation Reaction

Renni Zhao[a]; Rakesh Govind[a]; Naotsugu Itoh[b]
[a] Department of Chemical Engineering, University of Cincinnati, Cincinnati, Ohio [b] National Chemical Laboratory for Industry Ibaraki, Japan

To cite this Article Zhao, Renni , Govind, Rakesh and Itoh, Naotsugu(1990) 'Studies on Palladium Membrane Reactor for Dehydrogenation Reaction', Separation Science and Technology, 25: 13, 1473 — 1488
To link to this Article: DOI: 10.1080/01496399008050404
URL: http://dx.doi.org/10.1080/01496399008050404

SEPARATION SCIENCE AND TECHNOLOGY, 25(13-15), pp. 1473-1488 (1990)

STUDIES ON PALLADIUM MEMBRANE REACTOR FOR DEHYDROGENATION REACTION

Renni Zhao and Rakesh Govind*
Department of Chemical Engineering
University of Cincinnati
Cincinnati, Ohio 45221

Naotsugu Itoh
National Chemical Laboratory
for Industry
Ibaraki, 305 Japan

ABSTRACT

In current industrial practice dehydrogenation reactions require high temperatures and large amounts of inert (usually steam). Membrane reactors can be used to shift the equilibrium for these reversible reactions by removing products from the reaction zone. In this paper, experimental results will be presented for a palladium reactor system designed to investigate the feasibility of using palladium (Pd) alloy as the membrane material. Experiments have been conducted for isothermal and adiabatic conditions with air on the permeation side, wherein the oxygen reacts exothermically with the permeating hydrogen to decrease its partial pressure, thereby increasing its flux, and provide heat for the endothermic dehydrogenation reaction. Both theoretical and experimental results have been presented for dehydrogenation of 1-butene.

INTRODUCTION

In recent years, the use of membranes in reaction engineering has been recognized. By selectively separating the products from the reaction mixture, it is possible to achieve significant enhancement over equilibrium conversion. Shifting the thermodynamic equilibrium in this manner has

obvious industrial interest. It allows for reduced reaction temperatures, thereby minimizing side reactions and heating costs. Also, both reaction and separation may be achieved simultaneously in a single unit , making the membrane reactor a cost effective unit operation.

In this paper a computer simulation and experimental study are presented for a palladium membrane reactor system with an oxidation reaction on the permeation side and 1-butene dehydrogenation reaction on the reaction side. Palladium and its alloy membrane can not only withstand high temperature but also is permeable only to hydrogen and has catalytic activity for oxidation and dehydrogenation reactions. The oxidation reaction increases the reaction conversion as a result of hydrogen permeation through the membrane. Further, the coupling of an exothermic oxidation reaction with an endothermic dehydrogenation reaction allows effective heat transfer along the length of the reaction zone.

BACKGROUND

The phenomenon of hydrogen permeating through palladium was discovered by Thomas Graham[1] more than 100 years ago. Metallic palladium absorbs an unusually large amount of hydrogen. Hydrogen permeates through Pd-based membranes in the form of highly active atomic hydrogen which can react with other compounds absorbed on the catalyst surface.

One of the earliest applications of membranes to shift equilibrium was developed by Wood[2] (1960). He showed that by imposing a non-equilibrium condition on a hydrogen-porous palladium silver alloy membrane, an otherwise stable cyclohexane vapor is rapidly dehydrogenated to cyclohexene.

In recent years, the use of membranes for gas separation resulting in favorable chemical equilibrium shift has been recognized. Dokija *et at.*, Fukada *et al.*[3] and Kameyama *et al.*[4] employed porous vycor glass to selectively separate the hydrogen produced in the decomposition of hydrogen sulphide. Kameyama[5] showed the possibility of using porous alumina membrane. Raymont[6] suggested abundantly available hydrogen sulfide as a possible hydrogen source and discussed the possibility of using platinum or palladium alloy membranes to shift the equilibrium of the thermodynamically unfavorable decomposition reaction. Itoh *et al.*[7]

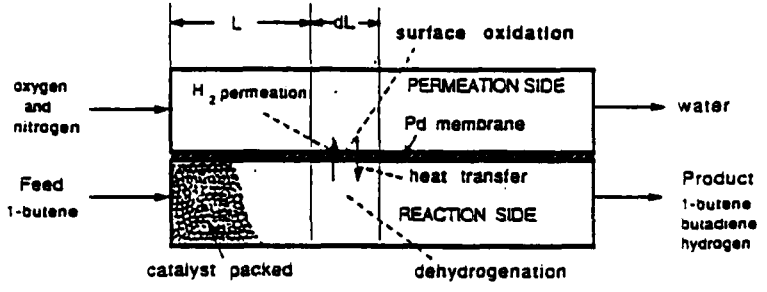

Figure 1. Schematic of a membrane reactor

studied dehydrogenation of cyclohexane in a palladium membrane reactor and showed that the removal of hydrogen by the membrane from the reaction mixture increased the conversion to as high as 99.5%.

In other works, Mohan and Govind [8][9] analyzed the effect of design parameters, operating variables, physical properties and flow patterns on membrane reactor performance. They have shown that for the case of dehydrogenation reactions with a hydrogen selective membrane, conversion comparable to those achieved with lesser permselective membranes can be attained at a substantially lower feed temperature. Ilias and Govind[10] have reviewed the development of high temperature membranes for membrane reactor application. Hsieh[11] has summarized the technology in the area of inorganic membranes.

The idea of coupling hydrogenation and dehydrogenation reactions in a catalytic membrane reactor was first proposed by Gryaznov *et al.* [12][13]. Recently, Itoh and Govind[14] have reported a theoretical study of coupling an endothermic hydrogen oxidation reaction with dehydrogenation of 1-butene in an isothermal palladium membrane reactor.

MODEL DEVELOPMENT

A schematic of a palladium membrane reactor is shown in Figure 1. The reversible reaction of 1-butene dehydrogenation occurs on the reaction side of the membrane in which the chrome-alumina catalyst is uniformly packed. The oxidation of hydrogen with oxygen in air occurs on the permeation or separation side of the palladium membrane surface. The palladium membrane acts as a catalyst for the oxidation reaction. The hydrogen produced by the dehydrogenation reaction permeates through the palladium membrane and then reacts with the oxygen on the permeation side. The dimensionless model equations governing the membrane reactor are essentially differential material and energy balances for each side of the membrane and are summarized as follows.

1. Mass balance

Reaction side (L>0)

$$\frac{dU_C}{dL} = -Da_r^0 exp\{\varepsilon_r(1-\frac{1}{\theta_r})\} f_r$$

$$\frac{dU_H}{dL} = Da_r^0 exp\{\varepsilon_r(1-\frac{1}{\theta_r})\} f_r - T_U^0 \, exp\{\varepsilon_p(1-\frac{1}{\theta_r})\}(\sqrt{\frac{P_{Hr}}{P_0}} - \sqrt{\frac{P_{Hs}}{P_0}})$$

$$U_D = 1 - U_C$$

$$U_I = DI_r \qquad (constant\ for\ inert\ gas)$$

Separation side (L>0)

$$\frac{dV_H}{dL} = T_U^0 \exp\{\varepsilon_p(1-\frac{1}{\theta_r})\}(\sqrt{\frac{p_{Hr}}{P_0}} - \sqrt{\frac{p_{Hs}}{P_0}}) - 2Da_s^0 \exp\{\varepsilon_s(1-\frac{1}{\theta_s})\} f_s$$

$$V_O = V_O^0 + (1 + U_H + V_H - U_C - U_H^0 - V_H^0)/2$$

$$V_w = 2(V_O^0 - V_O)$$

$$V_I = DI_s \quad (\textit{constant for inert gas})$$

2. Energy balance

Reaction side (L>0)

$$\frac{d(\sum_{i=1}^{4} C_{pi} U_i \theta_r)}{dL} = -Da_r^0 \exp\{\varepsilon_r(1-\frac{1}{\theta_r})\}\delta_r f_r + \Gamma(\theta_s - \theta_r)$$

Separation side (L>0)

$$\frac{d(\sum_{j=1}^{4} C_{pj} V_j \theta_s)}{dL} = -Da_s^0 \exp\{\varepsilon_s(1-\frac{1}{\theta_s})\}\delta_s f_s - \Gamma(\theta_s - \theta_r)$$

3. Initial conditions (L=0)

reaction side

$$U_C = 1, \quad U_I^0 = DI_r = \frac{u_I^0}{u_C^0}, \quad U_D = U_H^0 = 0, \quad \theta_r = 1$$

separation side

$$V_O^0 = \frac{v_O^0}{u_C^0}, \quad V_I^0 = DI_s = \frac{v_I^0}{u_C^0}, \quad V_W = V_H^0 = 0, \quad \theta_s = 1$$

4. Rate equations

reaction side

$$f_r = \frac{p_C^{1/2} - (p_D p_H / K)^{1/2}}{P_r^{1/2}(1 + 1.210\, p_C^{1/2} + 1.263\, p_D^{1/2})^2}$$

separation side

$$f_s = \frac{p_H^2 p_O}{P_s^3}$$

In this model the follow simplifying assumption have been made:

1. One-dimensional plug flow;
2. Negligible axial diffusion flux of heat and mass;
3. Negligible radial gradients of temperature and concentration;
4. Negligible pressure drop on either side of the membrane;
5. The heat and mass transfer resistances, aside from the permeation process itself, are negligible.

Plug flow conditions exist at high Reynolds numbers typically found in flow through packing or small radius tubes. In a permeator, the convective flow dominates over the diffusive flow i.e. a high Peclet number can be expected in a membrane reactor. Moreover, the pressure drop in a packed bed is usually a small fraction of the total pressure and can be neglected without significant error. To facilitate parametric analysis, the various design, operating, and physical parameters (membrane characteristics and dimensions, reactor dimensions, reaction side and separation side pressure, feed flow rate, inert gas flow rate, feed temperature, reaction rate constant, equilibrium constant, permeability) are included in the form of dimensionless groups. The three main dimensionless groups were: 1) Damkohler number, Da, for the reaction and separation sides, which is measure of the maximum forward reaction rate and is proportional to the membrane reactor length; 2) dimensionless group expressing the heat transfer coefficient across the membrane, Γ; and 3) dimensionless group containing the hydrogen permeability, Tu.

EXPERIMENTAL METHOD

In the experimental study, the reactor, schematically shown in Figure 2, consists of two separate rectangular parts with a 90 mm length, 25 mm width and 25 mm depth groove. The palladium membrane(100 mm × 33 mm and 0.025 mm thickness) held in place by two pieces of gasket which have a 80 mm × 20 mm rectangular hole in the center, is sandwiched

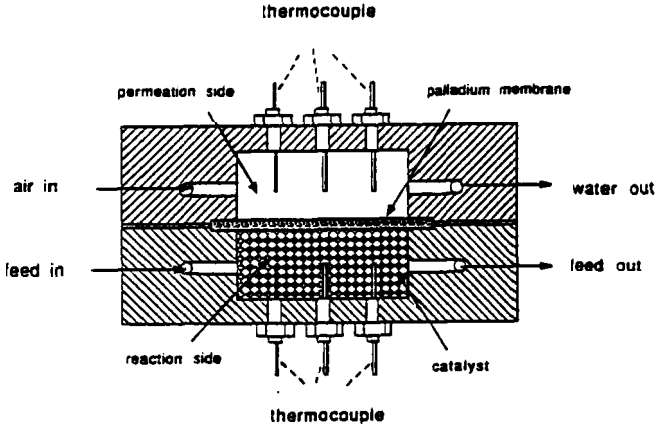

Figure 2. Schemtic of the experimental membrane reactor system

between the two reactor parts. Six thermocouples were located along the length of reactor to determine the temperature profile inside the reactor. The reversible reaction of 1-butene dehydrogenation occurred on the reaction side of membrane where chrome-alumina catalyst was uniformly packed. The oxidation of hydrogen with air occurred on the palladium surface on the other side of the membrane, referred to as the permeation (or separation) side. The palladium membrane acts as the catalyst during the oxidation. This surface oxidation reaction decreases the hydrogen concentration on the separation side , thereby increasing the permeation of hydrogen through the membrane. Further, more heat liberated by the exothermic oxidation reaction on the separation side flows across the membrane and facilitates the endothermic dehydrogenation reaction, thereby increasing its reaction rate.

A schematic of the experimental apparatus is shown in Figure 3. The feeds of 1-butene, argon, 10% oxygen and nitrogen mixture were supplied from gas cylinders . Each flow rate is measured by a mass flow meter. The down stream flow rate on the permeation side chamber is open to the atmosphere, thereby maintaining the permeation side at atmospheric pressure. The products of dehydrogenation and oxidation were analyzed using flame ionization detector (FID) or thermal conductivity detector (TCD) respectively. The detector signal was monitored by an on-line microcomputer.

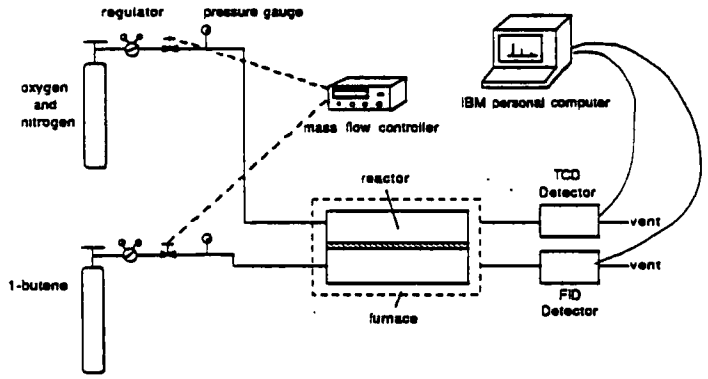

Figure 3. Schematic of the overall experimental apparatus

Measurement of reaction rate constant

The disappearance rate of 1-butene can be expressed by the following rate expression[15]:

$$r_r = k_f \Phi_d [p_C^{1/2} - (p_D p_H / K)^{1/2}]$$

where k_f, Φ_d and K are the reaction rate constant, adsorption term and the reaction equilibrium constant respectively. In this equation, p_C p_D and p_H are the partial pressures (atm) of the components involved.
The adsorption team Φ_d can be written as follows;.

$$\Phi_d = \frac{1}{(1 + 1.210\, p_C^{1/2} + 1.263\, p_D^{1/2})^2}$$

The reaction equilibrium constant, K, can be expressed as follows;

$$K = \frac{p_D p_H}{(p_{cis-2-butene} + p_{trans-2-butene} + p_{1-butene})}$$

The reaction equilibrium constant is calculated from thermodynamic data[16].

$$K = 1.94 \times 10^6 \exp[\frac{-15230}{T}] \qquad atm$$

The rate constant was independently measured by using a differential reactor packed with chrome-alumina catalyst particles. Before reaction, the catalyst was treated with 10 % oxygen gas mixture for 1 hour and then with argon for about half-hour at the reaction temperatures. This pretreatment is to regenerate the activity of the catalyst which had been deactivated due to coke deposition in the previous run. Either pure 1-butene or mixture of 1-butene and argon was fed into the reactor. The output stream was sampled and analyzed for the composition of the organic portion by a Perkin-Elmer 990 gas chromatograph equipped with a FID detector and a VZ-10 60/80 column(product of Alltech Associates, Inc.). The conversions were calculated based on the mole fraction of butadiene in the exit stream. This data was further analyzed to determine the rate constant. The experiment was carried out at several different input conditions and reaction temperatures. Figure 4 shows the Arrhenius plot of the obtained reaction rate constant for 1-butene dehydrogenation. The rate constant is given as follows :

$$k_f = 1.005 \times 10^3 \exp[\frac{-21600}{RT}] \qquad [mol/(h\,g\,atm^{1/2})]$$

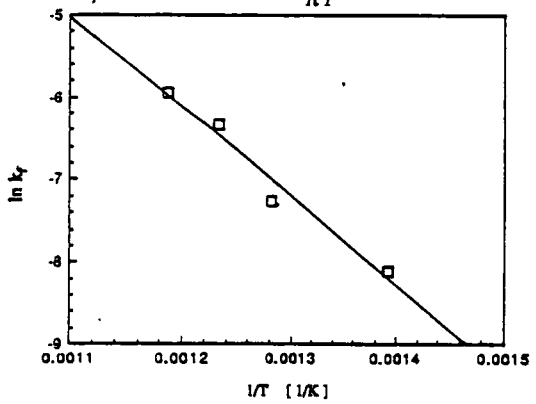

Figure 4. Arrhenius plot of the observed reaction rate constant versus the inverse of the temperature

For the case of determining the rate constant of hydrogen with oxygen on the palladium surface, direct reaction of oxygen and hydrogen takes place around 500 ^{0}C[17] and the reaction occurs mostly on the surface of the vessel. Leder and Butt [18] studied the reaction between hydrogen and oxygen at 100 ^{0}C with a dilute platinum catalyst. For investigating the oxidation reaction rate, hydrogen was fed into the reaction side. When the reactor had attained the reaction temperature, the exit valve on the reaction side was shut off, thereby allowing the hydrogen to permeate through the membrane. 10% O_2 and 90% N_2 mixture gas was introduced into the permeation side. The system pressure and flow rates were controlled and determined by mass flow meters. The products were analyzed by gas chromatograph with molecule sieve 5A column. Because of the catalytic effect of palladium and high temperature, the oxidation reaction was extremely fast. Hydrogen absorbed on the palladium surface reacted immediately due to the presence of oxygen. The results show that the exit hydrogen flow rate on permeation side is almost zero since the oxidation reaction was immediately completed. Hence, it can be assumed that the concentration of hydrogen on the permeation side is zero ($V_H = 0$) at the reaction operating condition and proper mixture flow rate.

Measurement of palladium membrane permeability

The permeation rate of hydrogen gas through the palladium membrane, Q_H, was assumed to obey the half-power pressure law[19]. The permeation flux of hydrogen through the membrane is proportional to the difference between the square root of the hydrogen partial pressures on the high and low pressure sides of membrane.

$$Q_H = A\, q\, [\,(P_H^h)^{1/2} - (P_H^l)^{1/2}\,]/Z$$

where q is the permeability of hydrogen through the membrane.

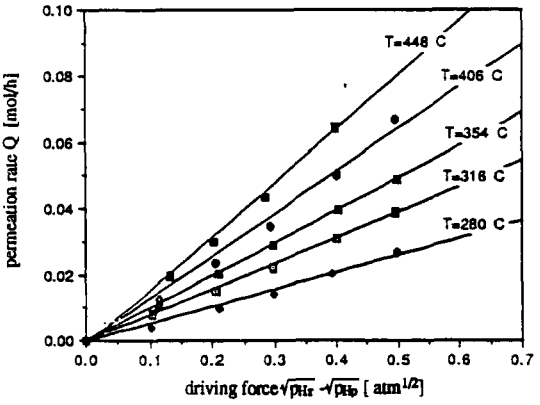

Figure 5. Permeation rate of hydrogen through the palladium membrane at different temperatures

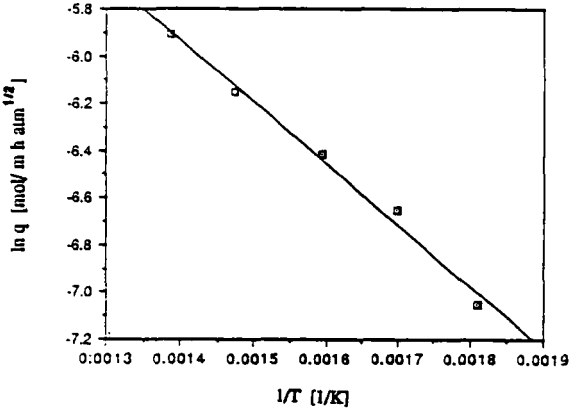

Figure 6. Permeability of hydrogen through the palladium membrane as a function of temperature

The hydrogen flow rate through the palladium membrane at various temperatures and differential pressures is shown in Figure 5. At a constant temperature, the permeation rate increases with increasing pressure differential across the membrane. In Figure 6, the permeability of hydrogen through the palladium membrane increases with temperature. The permeability of hydrogen through a palladium membrane can be expressed as follows:

$$q = 2.578 \times 10^{-5} exp\left[-\frac{2562.7}{T} \right] \qquad mol/(m\,s\,atm^{-1/2})$$

Membrane reactor operation

The membrane reactor was operated in two modes: 1) isothermal mode, in which the reactor was placed in a constant temperature furnace; and 2) adiabatic mode, in which the reactor was heated to the reaction temperature and then the furnace was switched off. Result of isothermal mode studies have been presented earlier[20].

In this paper, results have been presented for the adiabatic mode only. The operating conditions for the study were as follows:

1-butene feed flow rate	5 — 60 cm^3 /min
1-butene feed concentration	100%
flow rate on permeation side	20 — 60 cm^3 /min
oxygen feed concentration on permeation side	10%

Before starting the adiabatic run, both reaction and separation chambers were heated by hot gas containing 10% oxygen and 90% nitrogen. This allowed the catalyst to be regenerated due to the burning of coke deposited on the surface. When the reactor had attained the reaction temperature, the hot gas on reaction side was replaced by pure argon,

thereby allowing the oxygen to be purged from the reaction chamber. After ten minutes purging, the pure 1-butene feed was introduced into the reaction side and the system was kept running under isothermal operating condition for about ten minutes. After ten minutes, the furnace was turned off, and the exothermic heat from the permeation side was allowed to maintain the endothermic dehydrogenation reaction.

RESULTS AND DISCUSSION

For the case of isothermal operating condition, Figure 7 shows the simulation results of effect of inert gas flow rate on the membrane area and 1-butene conversion at fixed catalyst weight (1000g), reactant feed rate, $U_C^0 = 1.7 \times 10^{-5}$ mol/s ($=25$ cm^3/min), and reaction temperature 450 ^{0}C. For a fixed conversion, it can been seen that increasing the purge gas flow rate results in dramatically decreasing the membrane area in the reactor. This is due to the decreasing permeate partial pressure. The minimum membrane area required for a given conversion can be attained in the case of the oxidation reaction taking place on the membrane surface. Thus, using a coupled system of hydrogenation and dehydrogenation reactions occurring simultaneously on opposite surfaces of a membrane provides the maximum possibility of shifting dehydrogenation reaction conversion.

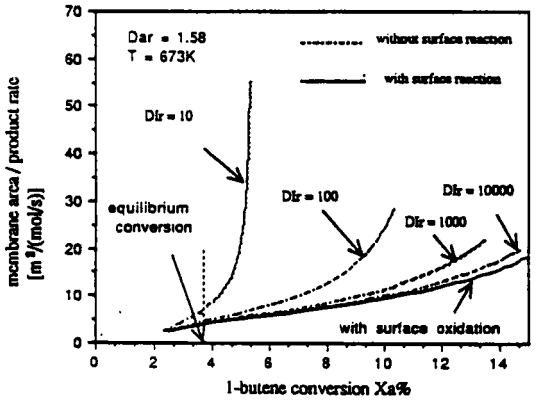

Figure 7 Effect of inert gas flow rate on the butene conversion and the required membrane surface area

For the adiabatic operating condition, Figure 8 shows the computer simulation result of the temperature profile within the reactor for a dimensionless heat transfer coefficient, $\Gamma = 0.1$, and $\Gamma = 10$. The temperature difference between reaction side and permeation side depends on the heat transfer coefficient. For high value of Γ, the temperature on the reaction side initially decreases since the reaction is endothermic. However, the heat released from the exothermic oxidation reaction dominates the endothermic heat effect. Hence, the temperature rises along the reactor length. The hydrogen concentration profile along the reactor length is shown in Figure 9. On the reaction side, there is a rapid increase in hydrogen concentration due to reaction. The exothermic reaction of hydrogen oxidation increases the temperature on the separation side and

accelerates the surface reaction of hydrogen with oxygen. The hydrogen on the separation side reacts immediately and the permeation rate increases sharply. Subsequently, the concentration of hydrogen on reaction side decreases. For high heat transfer rate through the membrane ($\Gamma = 10$), since the heat released by oxidation flows cross the membrane, the temperature and dehydrogenation rate on the reaction side increases. This increases the rate of dehydrogenation causing the hydrogen concentration to increase again at an intermediate point in the reactor. For a low heat transfer coefficient, the hydrogen concentration on the reaction side continues to decrease after an initial increase due to a decrease in the reaction temperature.

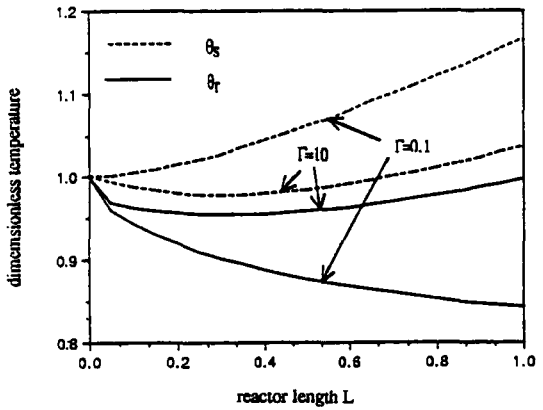

Figure 8 Temperature profiles in the reactor for the reaction and permeation side

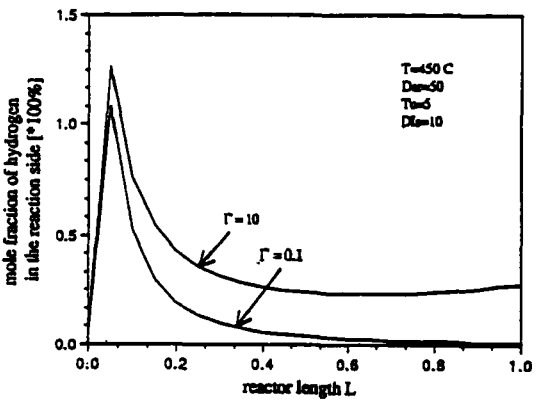

Figure 9. Concentration profiles of hydrogen along the reactor length for various heat transfer coefficients

The relation between conversion and the Damkohler number at different heat transfer coefficients is shown in Figure 10. For a fixed Damkohler number,Dar, improving the heat transfer coefficient can produce higher conversion. When Dar increases, the temperature on the reaction side decreases with the reaction. Thus the temperature drop blocks the dehydrogenation reaction. Finally the conversion increases slowly.

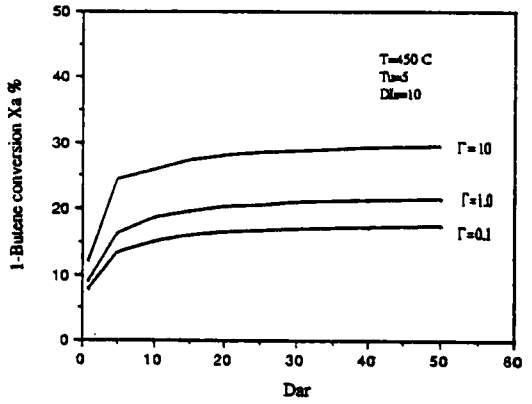

Figure 10. Relation between conversion and the Damkohler number for different heat coefficient dimensionless number

Figures 11 and 12 present the experimental results for an adiabatic operating condition. In this case, after the reactor had attained the required reaction temperature, the furnace was switched off and the heat of reaction from the oxidation reaction was allowed to drive the endothermic dehydrogenation reaction. Figure 11 shows the reaction side temperature as a function of time. It can be seen that the reaction temperature decreases from 450 ^{0}C to 388 ^{0}C in about 2 hours, indicating that the exothermic oxidation reaction heat was not sufficient for the endothermic dehydrogenation reaction. This was mainly due to the heat loss from the permeation or separation side to the environment through the reactor walls. Since the reactor was made from a solid block of stainless steel, there was sufficient heat capacity in the reactor walls to remove heat from the oxidation reaction side.

In Figure 12, the 1-butene conversion has been shown versus the feed flow rate for a adiabatic operation. The experimental results lie below the simulation results mainly due to heat losses from the oxidation reaction side. As the feed flow rate decreases, the 1-butene conversion increases due to increased residence time and permeation of hydrogen through the membrane.

It has been shown that while adiabatic operation is possible by coupling an exothermic oxidation reaction with an endothermic dehydrogenation reaction, the heat transfer between the reaction and permeation sides needs to be improved by possibly using a tube-and-shell arrangement, where the dehydrogenation reaction is conducted in the outer

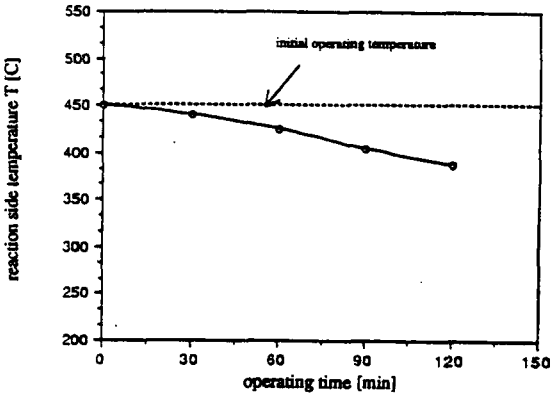

Figure 11. Reaction side temperature change with adiabatic operating time

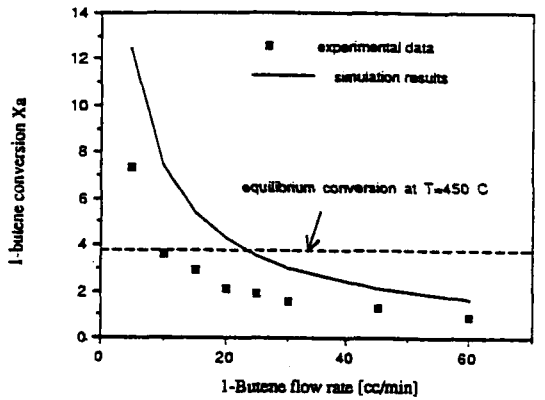

Figure 12. 1-butene conversion versus the feed flowrate for the adiabatic case at initial temperature of 450 C

shell side and the oxidation reaction on the tube side. Since a tube-and-shell reactor design would require a tubular palladium membrane, further research will concentrate on the development of technique for depositing a thin palladium film on porous tube surfaces.

CONCLUSION

The feasibility of the palladium membrane system with an oxidation reaction on the permeation side and 1-butene dehydrogenation reaction on the reaction side in a membrane reactor has been successfully demonstrated for application to catalytic dehydrogenation of 1-butene.

Heat transfer across the membrane from the exothermic oxidation reaction to the endothermic dehydrogenation reaction allowed conversion shift to be attained in the adiabatic case.

Nomenclature

A	membrane area m^2
$c_{p_c}^0$	specific heat of reactant at temperature T_0, cal/(mol·K)
c_{p_i}	specific heat of gas i at temperature T, cal/(mol·K)
C_{p_i}	dimensionless specific heat of gas i, $c_{p_i}/c_{p_c}^0$
Da_r^0	Damkohler number for reaction side at T_0, $k_f \cdot G \cdot P_r^{1/2}/u_c^0$
Da_s^0	Damkohler number for separation side at T_0, $k_s \cdot A \cdot P_s^3/u_c^0$
DI_r, DI_s	dilution ratio, u_i^0/u_c^0, v_i^0/u_c^0
E	activation energy, cal / mol
G	total weight of catalyst, g
h_0	overall heat transfer coefficient, cal /(m^2·s·K)
ΔH	heat of reaction cal/mol
k_f	rate constant of dehydrogenation, mol/(g-cat·h·$atm^{1/2}$)
k_s	rate constant of oxidation, mol/(m^2·h·atm^3)
K	equilibrium constant of dehydrogenation of 1-butene, atm
L	dimensionless reactor length
p_i	partial pressure of gas i, atm
p_{Hr}	partial pressure of hydrogen on reaction side, atm
p_{Hs}	partial pressure of hydrogen on separation side, atm
P_r	total pressure on reaction side, atm
P_s	total pressure on separation side, atm
P_0	reference pressure = 1 atm
q	permeability of hydrogen through palladium, mol/(m·h·$atm^{-1/2}$)
Q_H	permeation rate of hydrogen, mol/h
R	gas constant, cal/(mol·K)
T	absolute temperature, K
T_0	absolute temperature at inlet of reactor, K
Tu^0	dimensionless number relating hydrogen permeation at T_0 and P_0, $q \cdot A/(z \cdot u_C^0)$
u_i	flow rate of gas i in reaction side stream, mol/s
u_i^0	flow rate of gas i in reaction side inlet, mol/s
U_i	dimensionless flow rate of gas i in reaction side stream, u_i/u_c^0

U_H dimensionless flow rate of hydrogen in reaction side stream $u_H/(m \cdot u_c^0)$
v_j flow rate of gas j in separation side stream, mol/s
v_j^0 flow rate of gas j in separation side inlet, mol/s
V_j dimensionless flow rate of gas j in separation side stream, v_i/u_c^0
V_H dimensionless flow rate of hydrogen in separation side stream, $v_H/(m \cdot u_c^0)$
X_a 1-butene conversion, $(u_c^0-u_c)/u_c^0$
z thickness of membrane, m

Greek symbols

Γ $h_0A/(cp_c^0 u_c^0)$
δ $\Delta H/(c_{p_c}^0 T_0)$
ε $E/(RT_0)$
θ T/T_0 dimensionless temperature
ϕ_d adsorption denominator

subscripts

C reactant of dehydrogenation
D product of dehydrogenation
H hydrogen
i component i in reaction side stream
I inert
j component j in separation side stream
O oxygen
p permeation
r reaction side
s separation side
W water
0(zero) indicate $T = T_0$

superscripts

0(zero) indicate value at inlet condition
h high pressure side
l low pressure side

Literature Cited

1. Graham, T., Phil. Trans. Roy. Soc.(London). 156, 399 (1866).
2. Wood, J. B., J. Catalysis 11, 30 (1968).

3. Fukuda, K., Dokiya, M., Kameyama, T., and Kotera, Y., Ind. Eng. Chem. 17, 243 (1978).
4. Kameyama, T., Dokiya, M., Fujishige, M., Yokokawa, H., and Fukuda, K., Int. J. Hydrogen Energy 8, 5 (1983).
5. Kameyama, T., Dokiya, M., Fujishige, M., and Yokokawa, H., Int. Eng. Chem. Fund. 20, 97 (1981).
6. Raymont, M. E. D., Hydrogencarbon Process, 54, 139 (1975).
7. Itoh, N., AIChE. J. 33, 1576 (1987).
8. Mohan, K.,and Govind, R., AIChE. J. 34, 1493 (1988).
9. Mohan, K., and Govind, R., AIChE. J. 34, 1493 (1988).
10. Ilias. S.,and Govind, R., AIChE. Symposium Series 268, 18 (1989).
11. Hsieh, H. P.; AIChE. Symposium 268, 53 (1989).
12. Gryaznov, V. M., Smirnov, V. S., and Slinko, G., Catalysis; Hightower, J. W., Ed American Elsevier: New York, 1973.
13. Gryaznov, V. M., Platinum Metal Rev. 30, 68 (1986).
14. Itoh, N., and Govind, R., AIChE. Symposium Series 268, 10 (1989).
15. Happel, H., Blanck, H., and Hamill, T. D., I&EC Fund. 5, 289 (1960).
16. Aston, J. G., and Szasz, G. J., J. Chem. Phys. 14, 67 (1946).
17. Jacoson, Encyclopedia of Chemical Reaction; Reinholg Publishing: 1949; Vol. 3, p 625.
18. Leder, F., and Butt, J.B., AIChE. J. 12, 718 (1960).
19. Bohmholdt. G., and Wicke, E., Z. Physik. Chem. 56, 133 (1967).
20. Zhao,R., Itoh,N., and Govind, R., paper presented at the Annual ACS Meeting, Miami beach, FL, September 1989